

Influence of elastic scattering of photoelectrons on angle-resolved x-ray photoelectron spectroscopy

Kenji Kimura^{a)} and Kaoru Nakajima

Department of Micro Engineering, Kyoto University, Yoshida-honmachi, Sakyo, Kyoto 606-8501, Japan

Thierry Conard and Wilfried Vandervorst

IMEC, Kapeldreef 75, B-3001 Leuven, Belgium

(Received 1 June 2007; accepted 26 July 2007; published online 6 September 2007)

The validity of the electron effective attenuation length database developed by National Institute of Standards and Technology (NIST) is examined for x-ray photoelectron spectroscopy (XPS) measurement of HfO₂ (2.7 nm)/SiON (0.8 nm)/Si. The angular dependences of photoelectron yields are calculated using the NIST database and composition depth profiles measured by high-resolution Rutherford backscattering spectroscopy. The calculated result reproduces the observed XPS result fairly well even at larger emission angles up to 80°, indicating that the accuracy of XPS depth profiling can be improved using the NIST database. © 2007 American Institute of Physics. [DOI: 10.1063/1.2772769]

There is an increasing demand to analyze ultrathin films with high accuracy across many industries and research fields, especially in the microelectronics industry. Angle-resolved x-ray photoelectron spectroscopy (AR-XPS) is frequently used for this purpose. Recent development of high energy XPS has extended the analyzing depth up to 10 nm,¹ expanding the application field of AR-XPS. In the AR-XPS analysis, the escape probability of photoelectrons emitted at a certain depth without inelastic scattering, which is called the depth distribution function (DDF), is usually assumed as an exponential decay function with a decay constant equal to the inelastic mean free path (IMFP) for the photoelectrons. This simple assumption, however, is not correct due to elastic scattering. For accurate analysis, the effects of elastic scattering must be properly taken into account; i.e., the effective attenuation length (EAL) should be used instead of the IMFP.²

A database providing EALs has been published by the National Institute of Standards and Technology (NIST).³ The EALs were estimated from a solution of the kinetic Boltzmann equation within the so-called transport approximation.⁴ The calculated EAL is smaller than IMFP and is almost constant for emission angles θ_e less than $\sim 60^\circ$ and increases very rapidly when θ_e exceeds $\sim 60^\circ$.⁵ A careful measurement of EALs was conducted for Al $K\alpha$ -excited Si $2p$ photoelectrons in SiO₂ and Al₂O₃ to test the validity of the NIST database.⁶ The measured EAL for SiO₂ was 3.62 ± 0.13 nm at $\theta_e = 51.5^\circ$, which is about 93% of the IMFP calculated with the Tanuma-Powell-Penn (TPP-2M) formula⁷ and was in good agreement with the value (3.593 nm) predicted by the NIST database. Similar agreement was also observed for Al₂O₃, although the experimental EAL (2.71 ± 0.16 nm) was slightly smaller than the predicted value (2.853 nm). Thus, the NIST database is commonly believed to be reliable at least for emission angles less than 60° , while the validity at larger emission angles has not been examined yet.

Recently, the distinguishability of nitrogen composition profiles in SiON/Si by AR-XPS was studied by Powell *et*

*al.*⁸ They calculated N $1s$ peak intensities as a function of θ_e for five different N concentration distributions using an XPS spectrum-simulation tool.⁹ They found that appreciable difference in the N $1s$ intensity can be seen only at $\theta_e > 60^\circ$, indicating that detailed analysis at $\theta_e > 60^\circ$ is crucial for precise composition-depth profiling in AR-XPS. Thus, for depth profiling in AR-XPS, it is of great interest to see if the NIST database is reliable up to larger emission angles. In the present letter, we examine the validity of the NIST EAL database over a wide θ_e range up to 80° for HfO₂/SiON/Si. The observed AR-XPS results are compared with AR-XPS yields calculated with DDFs predicted by the NIST database. In this comparison, we need accurate composition depth profiles for calculation of AR-XPS yields. We employ high-resolution Rutherford backscattering spectroscopy (HRBS) for depth profiling because HRBS is one of the most reliable techniques for quantitative depth profiling with a subnanometer depth resolution.¹⁰

A thin SiON layer was prepared by a direct plasma nitridation on a cleaned Si(001) surface and, subsequently, a thin HfO₂ layer was grown on SiON/Si by atomic layer chemical vapor deposition at 300 °C. The nominal thicknesses of SiON and HfO₂ were 1.6 and 2.5 nm, respectively. The composition depth profiling was performed by HRBS using 400 keV He⁺ ion beam as a probe. The details of the HRBS measurement are described elsewhere.¹⁰ Briefly, energy spectra of He⁺ ions scattered at 50° were measured by a 90° sector magnetic spectrometer. In addition to the so-called random spectra, the [111] axial channeling spectra were measured to reduce the Si substrate signal. The channeling spectrum allows precise measurements of light elements, such as oxygen, nitrogen, and carbon.

Observed HRBS spectra are shown in the inset of Fig. 1. The composition depth profiles were obtained after a simulation of HRBS spectra and are shown in Fig. 1. The obtained profiles show the formation of an almost stoichiometric HfO₂ layer. The observed total amount of Hf is 7.5×10^{15} atoms/cm², which corresponds to 2.7 nm of HfO₂. The oxygen profile extends deeper than Hf and the nitrogen peak is seen in the same deeper region, indicating that there is an interfacial layer of SiON. Thus, except for a thin sur-

^{a)}Electronic mail: kimura@kues.kyoto-u.ac.jp

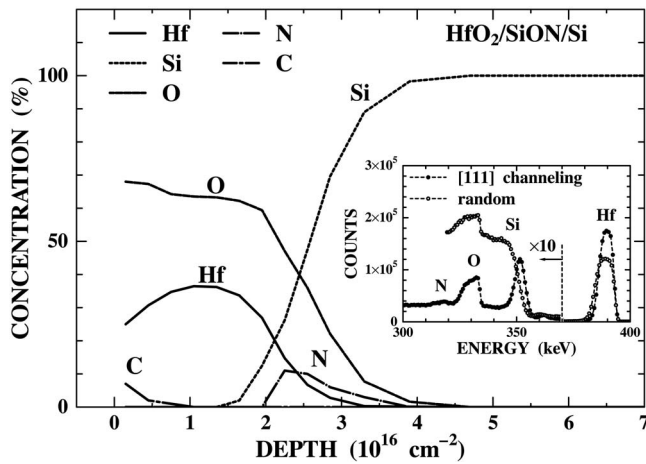


FIG. 1. Composition depth profiles of $\text{HfO}_2/\text{SiON}/\text{Si}$ measured by HRBS. The inset shows the observed HRBS spectra.

face contamination layer (3×10^{14} atoms/cm² of carbon), the observed profiles are in good agreement with the intended sample structure.

AR-XPS measurements were performed on a Thermo instrument equipped with an Al $K\alpha$ source. This instrument allows us to collect AR-XPS data in parallel without tilting the sample. Photoelectron spectra of Hf 4*f*, Si 2*p*, O 1*s*, and N 1*s* were measured at emission angles from 20° to 80° with respect to the surface normal. Shirley background subtraction and peak fitting were used when extracting peak areas. Figure 2 shows the observed photoelectron yield ratios, (Hf 4*f*)/(Si 2*p*), (O 1*s*)/(Si 2*p*), and (N 1*s*)/(Si 2*p*). Here, the Si 2*p* yield includes the signals from the substrate Si and the SiON film. The observed ratios, (Hf 4*f*)/(Si 2*p*) and (O 1*s*)/(Si 2*p*), increase with emission angle, indicating that both Hf and O exist at a shallower region than Si, while the ratio of (N 1*s*)/(Si 2*p*) is almost constant, indicating that nitrogen exists at a relatively deeper region. These results are qualitatively consistent with the HRBS profiles.

Photoelectron yields were calculated with a simple exponential decay function with a decay constant equal to the IMFP to examine the effect of the elastic scattering. Because

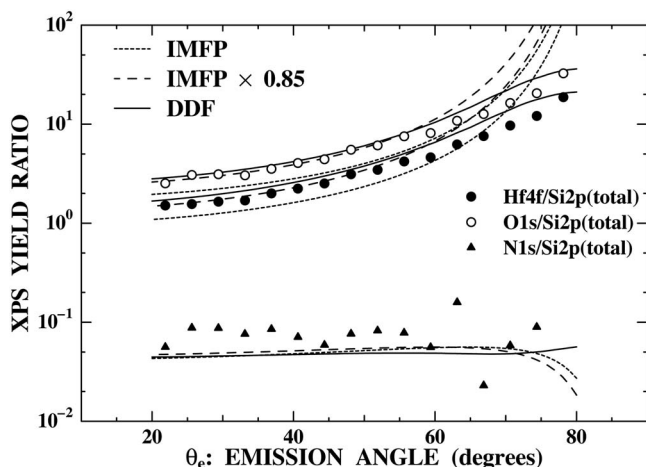


FIG. 2. Comparison between experimental (symbols) and calculated (lines) emission-angle dependences of XPS yields. The yield ratios (Hf 4*f*)/(Si 2*p*), (O 1*s*)/(Si 2*p*), and (N 1*s*)/(Si 2*p*) are shown. Calculated results with IMFP (dotted lines), modified IMFP (dashed lines) and DDF (solid lines), are shown.

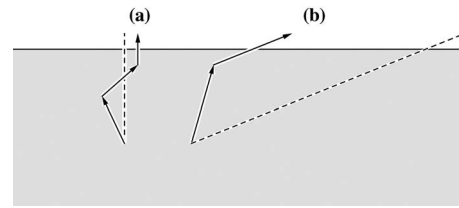


FIG. 3. Schematic illustration of the effects of elastic scattering at small emission angles (a) and large emission angles (b).

the composition is not uniform with depth, we used a composition-dependent IMFP defined by $\lambda_{\text{IMFP}} = 1/[\sum \sigma(A)N(A)]$, where $\sigma(A)$ and $N(A)$ are the inelastic cross section and the atomic density of element *A*, respectively. Inelastic-scattering cross sections of elements were estimated from the IMFPs for Si, SiO_2 , HfO_2 , and Si_3N_4 . The estimation of the inelastic cross section of Si is straightforward; i.e., $\sigma(\text{Si}) = 1/(\lambda_{\text{Si}}N_{\text{Si}})$, where λ_{Si} is the IMFP for Si and N_{Si} is the atomic density of Si. For other elements, the inelastic cross section of O, for example, was estimated by $\sigma(\text{O}) = [1/\lambda_{\text{SiO}_2} - \sigma(\text{Si})N_{\text{SiO}_2}(\text{Si})]/N_{\text{SiO}_2}(\text{O})$, where λ_{SiO_2} is the IMFP for SiO_2 and $N_{\text{SiO}_2}(\text{Si})$ and $N_{\text{SiO}_2}(\text{O})$ are atomic densities of Si and O in SiO_2 , respectively. Similar formulas, i.e., $\sigma(\text{Hf}) = [1/\lambda_{\text{HfO}_2} - \sigma(\text{O})N_{\text{HfO}_2}(\text{O})]/N_{\text{HfO}_2}(\text{Hf})$ and $\sigma(\text{N}) = [1/\lambda_{\text{Si}_3\text{N}_4} - \sigma(\text{Si})N_{\text{Si}_3\text{N}_4}(\text{Si})]/N_{\text{Si}_3\text{N}_4}(\text{N})$, were used for the estimation of the inelastic cross sections of Hf and N. In these calculations, the TPP-2M formula⁷ was employed for the estimation of IMFPs. This procedure provides simplistic estimates of the composition-dependent IMFPs. Precisely speaking, the IMFPs in compounds cannot be related to the inelastic-scattering cross sections of the constituent elements.¹¹ In the present case, however, this simple estimation gives rather good results because the specimen consists mainly of a stoichiometric HfO_2 film on a pure Si substrate.

In the calculation of photoelectron yields, the sample was divided into thin layers (thickness of each layer was 3×10^{15} atoms/cm²) and the IMFPs for each layer were calculated using the composition profile shown in Fig. 1. The results of the calculation are shown by dotted lines in Fig. 2. This calculation roughly reproduces the experimental results although the angular dependences of the yield ratios, (Hf 4*f*)/(Si 2*p*) and (O 1*s*)/(Si 2*p*), are somewhat steeper than the experimental data. If we reduce the IMFPs by 15%, better agreement can be obtained at emission angles smaller than 55° as shown by the dashed curves. This behavior is consistent with the previous experimental study, which indicated that the EAL for Si 2*p* photoelectrons in SiO_2 is smaller than the IMFP by 7% at $\theta_e = 51.5^\circ$.⁶ This reduction is attributed to the effect of elastic scattering. Due to elastic scattering, the actual path length becomes longer than the geometrical path length, as shown by Fig. 3(a). As a result, the EAL becomes smaller than the IMFP. This effect can be theoretically estimated by the NIST database. The DDFs for photoelectrons in HfO_2 were calculated by the NIST database using the TPP-2M formula at various emission angles. Figure 4 shows examples of the calculated DDFs for Si 2*p* photoelectrons as a function of the geometrical path length, $x/\cos \theta_e$. Essentially the same results are obtained for other photoelectrons of energy E_e if the path length is scaled by $E_e^{3/4}$. The DDFs can be approximated by an exponential decay function at $x/\cos \theta_e < 4$ nm irrespective of the emission angle. The decay constant for this exponential function is

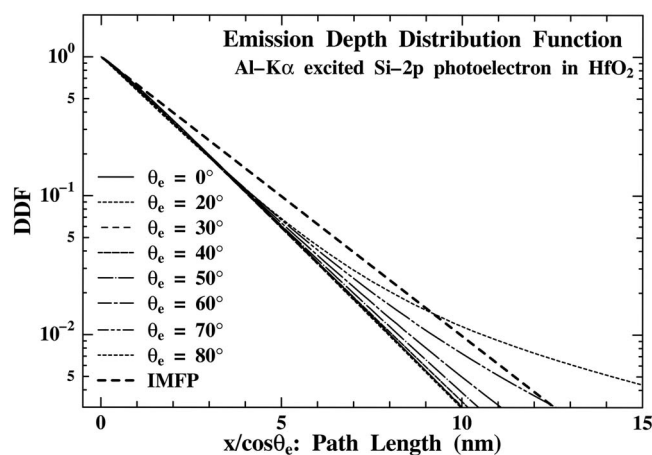


FIG. 4. Emission depth distribution functions for Si $2p$ photoelectrons excited by Al $K\alpha$ at different emission angles in HfO_2 calculated by the NIST EAL database with the TPP-2M formula. The result excluding elastic scattering is shown by a dashed line for comparison (IMFP).

1.86 nm, which is 86% of the IMFP (2.16 nm) indicating good agreement with the above obtained value of 85%. The relatively large effect compared to the previous result for SiO_2 [EAL is 93% of IMFP (Ref. 7)] can be ascribed to the larger elastic-scattering cross section of Hf. Thus, the effect of the elastic scattering can be taken into account by just reducing IMFP at $\theta_e < 55^\circ$. For precise depth profiling, however, analysis at $\theta_e > 60^\circ$ is crucial,⁸ and such a simple correction cannot reproduce the experimental results for large emission angles (see dashed curves in Fig. 2).

At larger θ_e , the DDF deviates considerably from the exponential decay function, as can be seen in Fig. 4. This is also the effect of elastic scattering. At larger emission angles, photoelectrons may escape from the surface by a shortcut, as shown by Fig. 3(b). This effect is pronounced for photoelectrons produced at deeper depths. Due to this effect, the escape probability of Si $2p$ photoelectrons, which are produced in a relatively deeper region than Hf $4f$ and O $1s$, is enhanced from a simple exponential decay function. As a result, better agreement between the experimental and calculated XPS yields could be obtained if DDFs are used instead of the simple exponential decay function. We now examine the extent to which DDFs predicted by the NIST database can improve the calculation of XPS yields.

The photoelectron yields calculated with the DDFs are shown by solid curves in Fig. 2. In the calculation, DDFs for photoelectrons in HfO_2 were used because the observed photoelectrons travel mainly in the HfO_2 layer. The agreement between the calculated and experimental results is improved

remarkably for (Hf $4f$)/(Si $2p$) and (O $1s$)/(Si $2p$) at $\theta_e > 60^\circ$. Good agreement over the whole angular region up to 80° is now obtained, indicating that the NIST database is reliable up to 80° . This allows AR-XPS analysis in a wide angular region and so more precise depth profiling in AR-XPS can be performed.

Finally, the relatively poor agreement between the experimental and calculated results for (N $1s$)/(Si $2p$) in Fig. 2 can be attributed to the errors in nitrogen analysis for both HRRBS and AR-XPS. Due to the small Rutherford cross sections and the overlapping of nitrogen signals with the substrate Si, the accuracy of nitrogen profiling in RBS is rather poor. In XPS measurements, quantitative analysis of N $1s$ peak in the present sample is also difficult because of the accidental interference by the plasmon loss of the Hf $4d$ peak.

In summary, the effect of elastic scattering in AR-XPS was experimentally studied for $\text{HfO}_2/\text{SiON}/\text{Si}$. The EAL is reduced from the IMFP by $\sim 15\%$ at $\theta_e < 55^\circ$, while it is increased at $\theta_e > 60^\circ$ due to elastic scattering. The observed AR-XPS result can be reproduced fairly well over a wide angular region up to 80° by simulations using DDFs predicted by the NIST EAL database.

The authors are grateful to T. Hattori, H. Nohira, S. Tanuma, and M. Suzuki for fruitful discussions. This work was supported by JSPS and FWO under the Japan-Belgium Research Cooperative Program and also supported in part by SENTAN, JST.

¹K. Kobayashi, M. Yabashi, Y. Takata, T. Tokushima, S. Shin, K. Tamasaku, D. Miwa, T. Ishikawa, H. Nohira, T. Hattori, Y. Sugita, O. Nakatsuka, S. Sakai, and S. Zaima, *Appl. Phys. Lett.* **83**, 1005 (2003).

²C. J. Powell and A. Jablonski, *Surf. Interface Anal.* **33**, 211 (2002).

³C. J. Powell and A. Jablonski, NIST Electron Effective Attenuation Length Database, Version 1.0, National Institute of Standards and Technology, Gaithersburg, MD, 2001.

⁴I. S. Tilinin, A. Jablonski, J. Zemek, and S. Hucek, *J. Electron Spectrosc. Relat. Phenom.* **87**, 127 (1997).

⁵A. Jablonski and C. J. Powell, *Surf. Sci. Rep.* **47**, 33 (2002).

⁶R. G. Vitchev, Chr. Defranoux, J. Wolstenholme, T. Conard, H. Bender, and J. J. Pireaux, *J. Electron Spectrosc. Relat. Phenom.* **149**, 37 (2005).

⁷S. Tanuma, C. J. Powell, and D. R. Penn, *Surf. Interface Anal.* **21**, 165 (1994).

⁸C. J. Powell, W. S. M. Werner and W. Smekal, *Appl. Phys. Lett.* **89**, 172101 (2006).

⁹W. S. M. Werner, W. Smekal, and C. J. Powell, NIST database for the simulation of electron spectra for surface analysis, SRD 100, National Institute of Standards and Technology, Gaithersburg, MD, 2005.

¹⁰K. Kimura, S. Joumori, Y. Oota, K. Nakajima, and M. Suzuki, *Nucl. Instrum. Methods Phys. Res. B* **219&220**, 351 (2004).

¹¹S. Tanuma, C. J. Powell, and D. R. Penn, *Surf. Interface Anal.* **25**, 25 (1997).